

# The Structural Context of Disease-causing Mutations in Gap Junctions\*<sup>§</sup>

Received for publication, June 15, 2006 Published, JBC Papers in Press, July 24, 2006, DOI 10.1074/jbc.M605764200

Sarel J. Fleishman<sup>†1,2</sup>, Adi D. Sabag<sup>§1</sup>, Eran Ophir<sup>§</sup>, Karen B. Avraham<sup>§</sup>, and Nir Ben-Tal<sup>‡3</sup>

From the <sup>†</sup>Department of Biochemistry, George S. Wise Faculty of Life Sciences, and <sup>§</sup>Department of Human Molecular Genetics and Biochemistry, Sackler School of Medicine, Tel-Aviv University, 69978 Ramat Aviv, Israel

Gap junctions form intercellular channels that mediate metabolic and electrical signaling between neighboring cells in a tissue. Lack of an atomic resolution structure of the gap junction has made it difficult to identify interactions that stabilize its transmembrane domain. Using a recently computed model of this domain, which specifies the locations of each amino acid, we postulated the existence of several interactions and tested them experimentally. We introduced mutations within the transmembrane domain of the gap junction-forming protein connexin that were previously implicated in genetic diseases and that apparently destabilized the gap junction, as evidenced here by the absence of the protein from the sites of cell-cell apposition. The model structure helped identify positions on adjacent helices where second-site mutations restored membrane localization, revealing possible interactions between residue pairs. We thus identified two putative salt bridges and one pair involved in packing interactions in which one disease-causing mutation suppressed the effects of another. These results seem to reveal some of the physical forces that underlie the structural stability of the gap junction transmembrane domain and suggest that abrogation of such interactions bring about some of the effects of disease-causing mutations.

Gap junction channels are formed by the docking of two hemichannels or connexons from adjacent membranes (1). Each connexon comprises six connexin subunits (2), proteins which are encoded by ~20 isoforms in the human genome (3). All connexins contain four transmembrane (TM)<sup>4</sup> segments (M1–M4), whose N and C termini are located in the cytoplasm (4). The channels are ~15 Å in diameter at their narrowest point (5), allowing the transport of ions and secondary messengers. They are expressed in nearly all vertebrate tissues and perform critical functions in mediating cell-to-cell signaling and metabolic coupling between apposed cells (6). Connexins

have been implicated in several diseases. For example, mutations in the gene encoding connexin 32 (Cx32; gene symbol *GJB1*) cause X-linked Charcot-Marie-Tooth disease, a common form of inherited motor and sensory neuropathy (7), and mutations in the gene encoding connexin 26 (Cx26; gene symbol *GJB2*) are responsible for a large proportion of cases of severe to profound non-syndromic hearing loss (8).

The structure of the gap junction has been solved only at intermediate resolution, revealing the approximate locations of each of the  $\alpha$ -helices comprising the TM domain (5) but not the locations of its constituent amino acids. As with many other human membrane proteins that lack bacterial homologs, structural analyses of connexins have been impeded by the absence of an atomic resolution structure (9). In particular, the effects of disease-causing mutations on gap junction structural stability have not been probed experimentally, and it has been difficult to design and interpret biochemical experiments on the structural aspects of connexins relating to individual amino acid residues. Instead, studies have focused on connexin domains (10–13), and normally, pairwise relationships among residues have not been detected other than by serendipity (14). However, based on the intermediate resolution structure (5) and computational inference methods (15, 16), a model of canonical  $\alpha$ -helices corresponding to the M1–M4 segments, which specifies the approximate positions of  $\alpha$ -carbons in the TM domain, was recently proposed (see Fig. 1) (17). Because the TM domain of connexins has been well conserved through evolution (17, 18), this model structure may serve as a template for all connexin isoforms, although the various isoforms are likely to exhibit slightly different helix-packing interactions. Hence, by specifying which residues are located in proximity to one another, the model can serve as a basis on which to formulate explicit hypotheses on interactions between amino acid positions.

We have studied several hypotheses of interactions between residue pairs by probing the localization of mutated human Cx26 and Cx32 that were C-terminally fused to green fluorescent protein (GFP) and expressed in HeLa cells that do not express endogenous connexins (19). Connexin trafficking to and insertion into the plasma membrane is dependent on several factors and processes, among them is the proper folding and oligomerization of the protein (20); substantial disruption of the protein stability could therefore result in mislocalized protein. We introduced single and double mutations into the connexin TM domain. A destabilizing mutation would show aberrant localization outside the plasma membrane. However, a carefully chosen second-site mutation could stabilize the mutated protein and retrieve the wild-type localization at the

\* This work was supported by the European Commission FP6 Integrated Project EUROHEAR, LSHG-CT-20054-512063, Israel Science Foundation Grant 222/04, and National Institutes of Health Grant R01 DC005641. The costs of publication of this article were defrayed in part by the payment of page charges. This article must therefore be hereby marked "advertisement" in accordance with 18 U.S.C. Section 1734 solely to indicate this fact.

<sup>§</sup> The on-line version of this article (available at <http://www.jbc.org>) contains supplemental data.

<sup>†</sup> These authors contributed equally to this work.

<sup>2</sup> Supported by a doctoral fellowship from the Clore Israel Foundation.

<sup>3</sup> To whom correspondence should be addressed. Tel.: 972-3-640-6624; Fax: 972-3-640-6834; E-mail: nirb@tauex.tau.ac.il.

<sup>4</sup> The abbreviations used are: TM, transmembrane; Cx, connexin.

sites of cell-cell apposition. This procedure is similar in spirit to the double-mutant cycle (21) and to second-site suppression assays (22). In all of these analyses, if the phenotypic effects of one mutation are found to depend on whether or not the other is mutated as well, this will indicate that the two amino acid sites interact (23). It should be noted that these experimental assays cannot, on their own, distinguish between direct physical interactions of a pair of positions and indirect interactions mediated via other residues (24). However, the model structure, although approximate, helped us to constrain the possible explanations. Based on the results of the mutation analyses, we identified the most likely justification for the observed phenotypes by computing approximate models of the side chains of interacting residues. We thus detected, for the first time, interactions that apparently stabilize contacts between TM helices in connexins; abrogation of these interactions leads to aberrant phenotype and disease.

## EXPERIMENTAL PROCEDURES

In general, we followed the experimental procedures presented in Ref. 37.

**Cloning**—Genomic DNA of each of the genes, *GJB2* (Cx26) and *GJB1* (Cx32), was double-digested with HindIII and KpnI and cloned into a pEGFP-N1 expression vector (Clontech, Palo Alto, CA).

**Mutant Connexin Expression Constructs**—Mutations were introduced into the open reading frame of human *GJB1* and *GJB2* genomic DNA (subcloned into a pEGFP plasmid) by PCR site-directed mutagenesis using the QuikChange kit (Stratagene, La Jolla, CA). DNA extracted from single colonies was sequenced at the Tel-Aviv University Sequencing Unit (Faculty of Life Sciences) using the ABI 377 DNA sequencer (PE Biosystems, Foster City, CA). A DNA template of one single mutation of each set of mutations was used with the mutagenic primers of the second mutation in the same set to generate the double mutants.

**Cell Cultures and Transfections**—Communication-deficient HeLa cells, which do not express endogenous connexins, were kindly provided by Prof. David Kelsell (University of London). The cells were grown in low-glucose Dulbecco's modified Eagle's medium supplemented with 10% fetal-calf serum, antibiotics (100  $\mu$ l/ml penicillin/streptomycin), and glutamine (290  $\mu$ l/ml) in a humidified atmosphere containing 5% CO<sub>2</sub> at 37 °C. The cells were plated onto six-well plates on coverslips and incubated for 24 h to 60–70% confluence.

HeLa cells were transiently transfected using Lipofectamine 2000 (Invitrogen) according to the manufacturer's instructions with modifications. The amount of reagent was reduced by half and incubated mixed with an equal volume of Neowater (DoCoop Technologies, Or Yehuda, Israel) for 5 min at room temperature. This mixture and plasmid DNA were incubated separately in OptiMEM for 5 min and combined for another 20 min at room temperature. HeLa cells (60–70% confluence) were washed with OptiMEM and incubated with the combined Lipofectamine/plasmid DNA solution at 37 °C. After five hours, the transfection medium was removed from the cells to prevent toxicity, and cells were incubated in medium without antibiotics overnight.

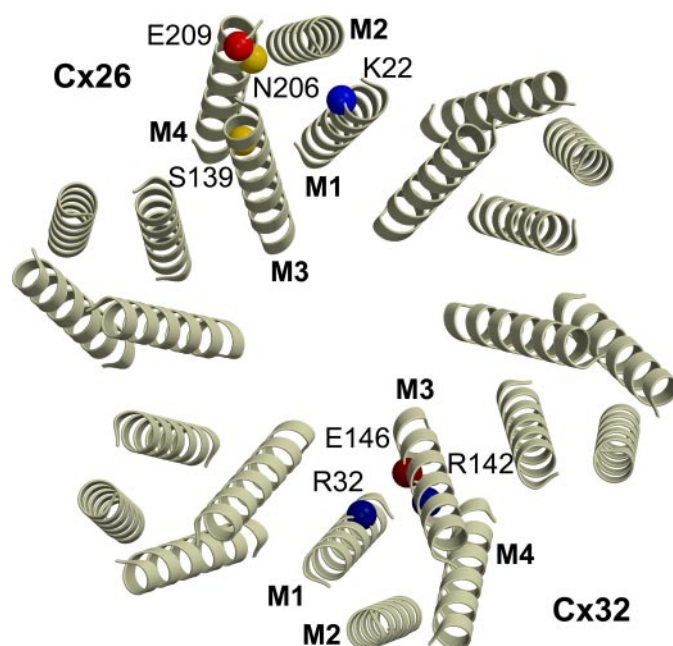


**FIGURE 1. Overall organization of the gap junction TM domain in one of two apposed membranes viewed from the cytoplasm of one cell looking toward the gap.** Six connexin subunits are organized around a central pore. The model structure (Protein Data Bank code 1txh) (17) reports only the positions of  $\alpha$ -carbons, assuming that each TM segment forms a canonical  $\alpha$ -helix. The model guided the mutation analyses by suggesting which residues form physical interactions. Amino acid positions that were mutated in Cx26 (top) and Cx32 (bottom) are indicated by spheres. Blue and red spheres represent the positions of positively and negatively charged amino acids, respectively; yellow spheres represent polar residues. One-letter codes for the amino acids are shown: E, Glu; K, Lys; N, Asn; R, Arg; and S, Ser. This and all other molecular representations were generated using MOLSCRIPT (38) and rendered with Raster3D (39).

**Cellular Localization**—Cells were fixed with either 4% paraformaldehyde for 20 min or with 100% ethanol (–20 °C) for 5 min and mounted on slides using Gel Mount (Biomedica, Foster City, CA). A comparison of the phenotypes using either fixation agent revealed no observable differences (data not shown). The data presented in the paper are based on paraformaldehyde as the fixation agent, as was done, e.g. in Refs. 14 and 37. Slides were observed through a Leica TCS SP2 AOBs confocal microscope. For each of the fluorescence images shown here, we examined the phase-contrast image to identify the regions of apposition between cells. The phase-contrast and fluorescence images are available as supplemental data.

**Structural Modeling**—The template structure of the TM domain of the gap junction, comprising Cx32 monomers (Protein Data Bank code 1txh) (17), was used as a starting point. Backbone atoms were added to this model using the Biopolymer module of the InsightII program (Accelrys, San Diego, CA). The sequences of Cx26 and Cx32 were aligned (17) to generate a model of the gap junction formed by Cx26 monomers. Side chains were then added to both structures using default parameters. Steric clashes were ignored at this stage. The rotameric states of Lys-22 (Cx26), Arg-32, and Arg-142 (Cx32) were examined manually, and rotamers were selected that minimized distances from the putative salt bridge partners, while also minimizing steric clashes with other parts of the protein.

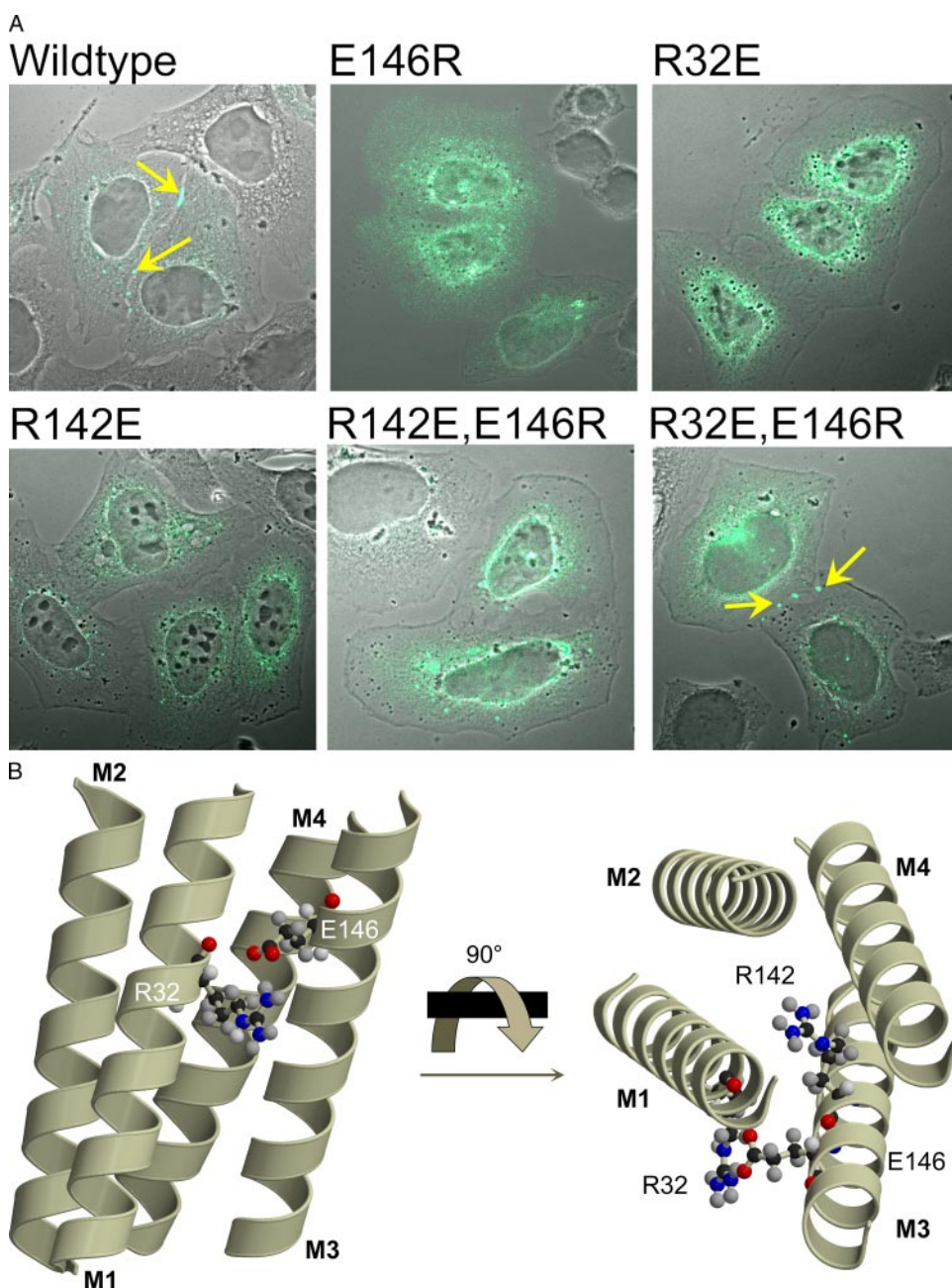


FIGURE 2. *A*, charged amino acids at the interface between the pore-lining helices M1 and M3 of Cx32 were mutated singly and doubly. Localization assays show that the two single charge reversals are mislocalized (top). The R32E/E146R double mutant restores membrane localization (yellow arrows), indicating that these positions interact. Pictures were taken by confocal microscopy. For each field, three images were taken: phase contrast, to show the boundaries of the cells, green fluorescence, to show the expression of the connexin-GFP chimera protein and a merge of the two, to verify the localization of gap junction plaques in the plasma membrane in points of cell-cell apposition. The phase-contrast and fluorescence images for all figures presented in the manuscript are available as supplemental data. *B*, the modeled side chains suggest that only the paired residues Arg-32/Glu-146 could form a salt bridge without invoking severe steric clashes, as shown by the localization assays. Because the localization assays (*A*) did not detect interactions between Arg-142 and other residues, this modeled side chain (shown on the right) should be considered as speculative.

## RESULTS

**A Salt Bridge between the M1 and M3 Pore-lining Helices**—A region of the model structure that showed particular promise for this approach was the interface between the M1 and M3 pore-lining helices, where a triad of charged positions (Arg-32, Arg-142, and Glu-146 of Cx32) is located (Fig. 1). These three positions (the first two occupied by basic residues and the last by an acidic resi-

due) are highly conserved throughout all connexins. In theory, the Arg and Glu residues, which are reciprocally charged and are near the water-filled pore lumen, could be involved in stabilizing electrostatic interactions; it has been estimated that salt bridges embedded in water can add nearly 1 kcal/mol to protein stability (25, 26).

We investigated the possible existence of an interaction between Arg-32 and Glu-146 by reversing the charges of these positions singly and doubly in Cx32 (Fig. 2*A*) (Table 1). Both single mutants, R32E and E146R, were localized outside the plasma membrane, which might be indicative of protein misfolding. Interestingly, a similar charge-reversing mutation, E146K in Cx32, was implicated in Charcot-Marie-Tooth disease (27). Remarkably, the double mutant R32E/E146R, which re-establishes charge complementarity between M1 and M3, restored membrane localization. The compensation suggests that the two residues interact. Given the model structure, it is likely that this interaction involves a salt bridge that stabilizes the interface between M1 and M3 (Fig. 1).

We also investigated the existence of an alternative interaction between Arg-142 and Glu-146. Here too, both single mutants were mislocalized. Despite the proximity between positions 142 and 146, however, the R142E/E146R double mutant did not elicit wild-type localization.

To explain this pattern of phenotypes, we examined the connexin model structure and explored the possible rotameric states (*i.e.* conformations) of the side chains of Arg-32, Arg-142, and Glu-146 (Fig. 2*B*). One of the rotamers of Arg-32 complied with the formation of an interhelical salt bridge with Glu-146. By contrast, none of the potential rotameric states of the side chain of Arg-142 could interact with Glu-146 without gener-

ating steric clashes with other parts of the protein. Hence, guided by the mutation assays, modeling of the side chains provided putative mechanistic explanations of the observed localization phenotypes. However, it should be borne in mind that this explanation is based on the model that the localization assay is attempting to support and that correct modeling of side chains is highly sensitive to the accuracy of the C- $\alpha$  model structure (28).

**TABLE 1****Frequency of coupled cells transfected with wild-type and mutated connexins**

Means and S.D. for each connexin were computed on the basis of three separate experiments and normalized to the levels in the wildtype. For each entry at least 250 transfected cells were counted. Transfection efficiencies in each case were at least 40%. All mutants that showed any coupling (>0%) were statistically indistinguishable on a two-sided *t*-test from the coupling levels in their respective wildtype protein ( $\alpha = 5\%$ ). NA, not applicable.

	Frequency of coupled pairs	S.D.
<b>Cx32 constructs</b>		
Wild type	1	0.06
R32E	0	NA
R142E	0	NA
E146R	0	NA
R142E/E146R	0	NA
R32E/E146R	0.97	0.11
<b>Cx26 construct</b>		
Wild type	1	0.21
K22E	0.75	0.27
E209K	0	NA
K22E/E209K	0.55	0.39
N206S	1.13	0.11
S139N	0	NA
N206S/S139N	1.15	0.09

Although wild-type connexins are membrane-localized, our images show fluorescence also outside the membrane, even in wild-type connexin (e.g. Fig. 1). Localization of wild-type connexins outside the membrane, in addition to the existence of gap junction plaques, have been observed in other studies involving overexpressed connexins, and it has been suggested that the cytoplasmic fraction of the protein is at least in part localized in aggresomes (29). The important point to notice from the perspective of the current study is that, along with the localization of some of the protein in the cytoplasm, wild-type and doubly mutated connexins are localized in the plasma membrane, whereas the single mutants are not.

*A Salt Bridge at the Intercellular Part of the TM Domain*—The charged residues of another pair, Lys-22 (M1) and Glu-209 (M4) of Cx26, face one another in the model structure, potentially forming a salt bridge (Fig. 1). These positions are conserved throughout the connexin family to basic and acidic identities, respectively. Mutations in both positions of the homologous Cx32 were implicated in Charcot-Marie-Tooth disease (30, 31). Our results show that, in Cx26, the single mutant E209R is mislocalized (Fig. 3A), similar to the disease-causing mutation to Lys in the homologous Cx32 (30). By contrast, K22E was properly localized in the plasma membrane (Table 1). The double mutant K22E/E209R rescued the aberrant localization phenotype of E209R and restored wild-type localization in the plasma membrane, suggesting that the two positions interact probably through an interhelical salt bridge. However, the normal localization of K22E, where no salt bridge can be formed, suggests that additional forces contribute to stabilization of this region. We did not detect similar compensation when testing this double mutant in Cx32 (data not shown), possibly because of subtle sequence and structure differences between these isoforms (Lys-22 in Cx26 is aligned with Arg-22 in Cx32). It is nevertheless very likely that the overall structure and salt bridge interactions present in Cx26 are also present in Cx32 (17, 18). It should be noted that, although compensation is a sign of physical interaction, lack of compensation

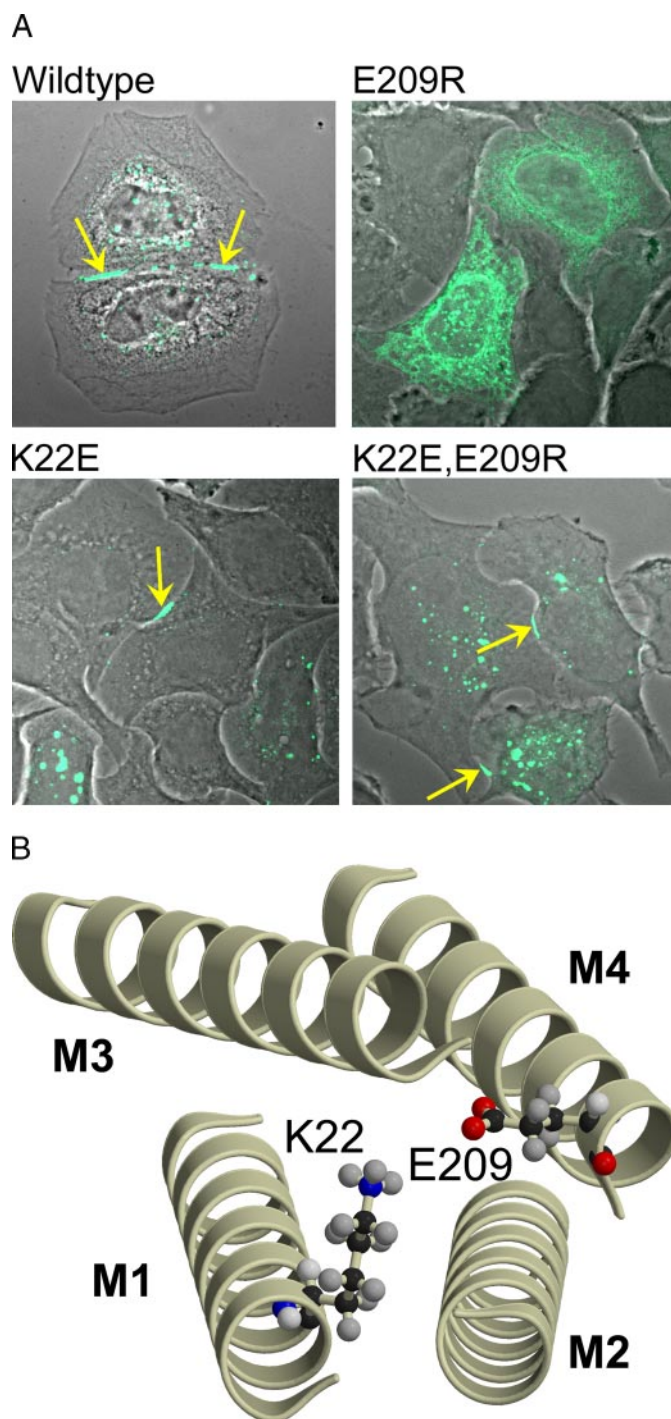


**FIGURE 3.** A, localization assays of wild-type, singly mutated, and doubly mutated Cx26 fused to GFP and expressed in HeLa cells. The single mutants E209R and K22E are cytoplasm- and membrane-localized, respectively. The mutation K22E suppresses the aberrant phenotype of E209R, indicating that the two positions interact. B, Lys-22 (M1) and Glu-209 (M4) of Cx26 may form a salt bridge. The two positions are located on the cytoplasmic boundary of the presumed hydrophobic core of the membrane and may thus be embedded in water or in the vicinity of the polar headgroups. The distance between the modeled amino and carboxyl moieties is <math>< 5 \text{ \AA}</math>.

(as in Cx32) does not necessarily indicate that the residues are remote (discussed in Refs. 32 and 33).

Further examination of the model structure in light of the results of the localization assay revealed one choice of rotamers for the modeled side chains of Lys-22 and Glu-209, where the car-

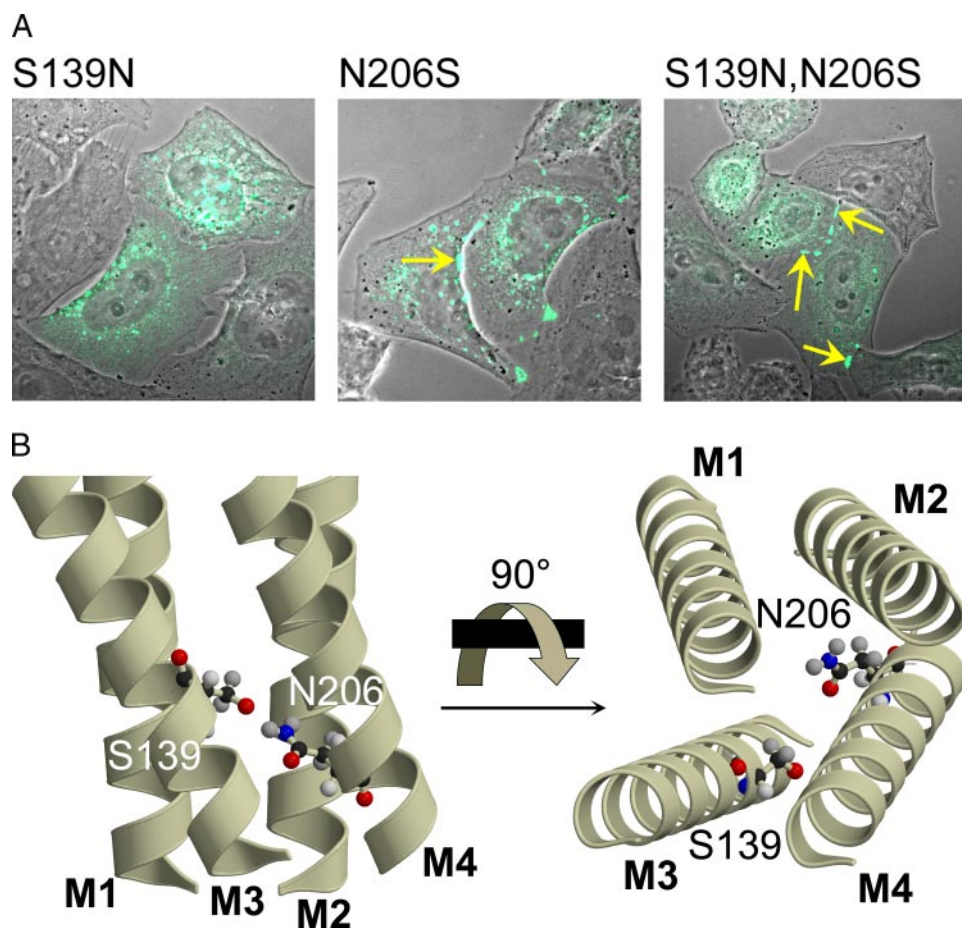


FIGURE 4. *A*, of the two mutations that cause deafness, S139N and N206S in Cx26, only the first is mislocalized. The second mutation compensates for the effects of the first, restoring the wild-type localization. The wild-type localization phenotype of Cx26 is shown in Fig. 3*A*. *B*, Ser-139 and Asn-206 of Cx26 are too far apart (roughly 6–7 Å) to interact directly. They can, however, interact through other residues in their vicinity.

boxyl and amino moieties of the side chains could point toward one another and are roughly 4–5 Å apart (Fig. 3*B*). The two positions are located at the end of the presumed hydrophobic core of the membrane on the cytoplasmic side (Fig. 1) and thus are likely to be exposed to the polar headgroups and the water in this environment. Embedded in water, this salt bridge is also expected to have stabilizing energetic effects on the folding of the protein (25, 26). It is instructive that the model structure provides a framework for understanding why one of the single mutants has deleterious effects on stability, whereas the other does not (Fig. 3*A*). The E209R mutation not only replaces the charge in this position but also adds to the side chain length, destabilizing the structure by bringing a positive charge from position 209 into the vicinity of the endogenous positively charged Lys-22 as well as by adding the potential for forming steric clashes. The compensating K22E mutation places two negative charges in the same region. However, because of the significant length difference between the side chains of Lys and Glu, the charges are more distant from one another in comparison to the distance between these residues in the wild type, reducing the effects of same-charge repulsion. By contrast, the above-mentioned Arg→Glu mutations in positions 32 and 142 did not show wild-type localization (Fig. 2*A*). The model offers an explanation for this difference in phenotypes as well. Whereas the interface between Arg-32 and Glu-146 on the

pore-lining helices M1 and M3 is quite tight (Fig. 2*B*), increasing the effects of same-charge repulsion, the interface between M1 and M4, where positions Lys-22 and Glu-209 are located, is less tight (Fig. 3*B*).

*One Disease-causing Mutation Compensates for the Aberrant Localization Phenotype of Another—*Another pair of residues, Ser-139 (M3) and Asn-206 (M4) of Cx26, is particularly relevant because of its involvement in a genetic disease (34, 35). Mutations in these two amino acids also demonstrate a pattern of localization phenotypes suggestive of an interaction. Theoretically, interactions between these polar positions could result from hydrogen bonding or steric packing (Fig. 1). The localization assays showed that the S139N mutant was mislocalized, whereas N206S exhibited wild-type localization (Fig. 4*A*) (Table 1), although altered voltage-gating properties in this latter mutant have been reported (36). Interestingly, both of these mutations were implicated in non-syndromic hearing loss (34, 35). When this pair is doubly mutated, however, one disease-causing mutation compensates for the effects of the other, restoring wild-type localization (Fig. 4*A*). Although the model sug-

gests that the two residues are oriented toward one another (Figs. 1 and 4*B*), the modeled side chains do not appear to be in direct contact (~6–7 Å apart). This is mainly because of a difference in the register along the axis vertical to the plane of the membrane, precluding the formation of a hydrogen bond. Hence, interpretation of the localization assay in light of the model suggests that the interaction between these residues results from packing with intermediate amino acid positions (24). Whereas the S139N mutation adds to the volume at the interface between helices M3 and M4, resulting in mislocalization, the N206S mutation compensates for this increased volume and restores membrane localization in the double mutant.

## DISCUSSION

Lack of an atomic resolution structure of the gap junction has made it extremely difficult to conduct biochemical investigations within a consistent framework (9). Here, we used a model based on an intermediate resolution structure (17) to formulate testable hypotheses to uncover some of the physical forces underlying the stability of the connexin TM domain at the molecular level. When use of this model is coupled with carefully planned mutagenesis, competing structural explanations may be resolved and mechanistic understanding improved.

Second-site suppression assays need to strike a fine balance

between the dual goals of introducing a mutation radical enough to elicit an aberrant phenotype, on the one hand, but one that does not cripple the protein so completely as to preclude its rescue by a second-site mutation, on the other hand. Thus, two of the three sets of mutants targeted positions that are situated in spacious regions of the model structure (Arg-32 and Glu-146 of Cx32; and Arg-22 and Glu-209 of Cx26), where they are not expected to induce extensive changes to the packing of the helices. In these sets, we used radical charge-reversal substitutions. In another set of mutants, involving positions that are packed inside the core of the helix bundle (Ser-139 and Asn-206 of Cx26), we tested substitutions that were physicochemically mild to reduce the chances that they would bring forth global changes to the protein structure. In all of these sets, clinical and some biochemical data suggested that the effects of the mutations would be observable in our assays.

Based on compensation assays, we suggested atomic models for several amino acid residues, thus refining the structural model of the gap junction TM domain, which specified only the locations of  $\alpha$ -carbons (17). It is notable that, since the publication of the intermediate resolution structure of the gap junction in 1999 (5), it has not been supplanted by an experimental atomic resolution structure. Systematic compensation studies could thus provide constraints that specify the nature of the interactions between amino acid residues on apposed helices. In particular, using experimental assays (13) such as electrophysiology and dye-transfer, it may be possible to test mutations that involve more subtle physicochemical changes than those attempted here, including mutations that only change the steric properties of the side chain, e.g. Val $\rightarrow$ Ile. Based on such studies, it might be possible to provide an atomic resolution description of much of the connexin TM domain, circumventing, in part, the impediments to obtaining an experimental atomic resolution structure (9).

Here, we have focused on connexin localization, and the capacity of doubly mutated connexins to form functional gap junctions that conduct ions, secondary messengers, metabolites, etc., should also be examined. Intriguingly, the three sets of compensatory mutations reported here indicate that elimination of specific interhelical contacts might be the cause of a number of connexin-related genetic diseases. The fact that the localization phenotype can be restored by second-site mutations suggests that it might be possible to rescue the aberrant localization of some mutated connexins by applying small molecules that stabilize the structure of the TM domain.

*Acknowledgments*—We thank Prof. A. Horovitz, Prof. F. Mammano, Dr. V. H. Hernandez, Prof. B. J. Nicholson, Dr. Y. Ofran, Prof. G. Schreiber, T. Sobe, Prof. V. M. Unger, and Dr. O. Yifrach for comments and suggestions, Prof. D. Kelsell for HeLa cells, and Drs. L. Mittelman and A. Barbul for confocal microscopy.

## REFERENCES

- Kumar, N. M., and Gilula, N. B. (1996) *Cell* **84**, 381–388
- Cascio, M., Kumar, N. M., Safarik, R., and Gilula, N. B. (1995) *J. Biol. Chem.* **270**, 18643–18648
- Willecke, K., Eiberger, J., Degen, J., Eckardt, D., Romualdi, A., Guldenagel, M., Deutsch, U., and Sohl, G. (2002) *Biol. Chem.* **383**, 725–737
- Milks, L. C., Kumar, N. M., Houghten, R., Unwin, N., and Gilula, N. B. (1988) *EMBO J.* **7**, 2967–2975
- Unger, V. M., Kumar, N. M., Gilula, N. B., and Yeager, M. (1999) *Science* **283**, 1176–1180
- Pitts, J. D. (1998) *BioEssays* **20**, 1047–1051
- Bergoffen, J., Scherer, S. S., Wang, S., Scott, M. O., Bone, L. J., Paul, D. L., Chen, K., Lensch, M. W., Chance, P. F., and Fischbeck, K. H. (1993) *Science* **262**, 2039–2042
- Kelsell, D. P., Dunlop, J., Stevens, H. P., Lench, N. J., Liang, J. N., Parry, G., Mueller, R. F., and Leigh, I. M. (1997) *Nature* **387**, 80–83
- Fleishman, S. J., Unger, V. M., and Ben-Tal, N. (2006) *Trends Biochem. Sci.* **31**, 106–113
- Kronengold, J., Trexler, E. B., Bukauskas, F. F., Bargiello, T. A., and Verselis, V. K. (2003) *J. Gen. Physiol.* **15**, 389–405
- Hu, X., and Dahl, G. (1999) *FEBS Lett.* **451**, 113–117
- Trexler, E. B., Bukauskas, F. F., Kronengold, J., Bargiello, T. A., and Verselis, V. K. (2000) *Biophys. J.* **79**, 3036–3051
- Harris, A. L. (2001) *Q. Rev. Biophys.* **34**, 325–472
- Skerrett, I. M., Aronowitz, J., Shin, J. H., Cymes, G., Kasperek, E., Cao, F. L., and Nicholson, B. J. (2002) *J. Cell Biol.* **159**, 349–360
- Fleishman, S. J., Harrington, S., Friesner, R. A., Honig, B., and Ben-Tal, N. (2004) *Biophys. J.* **87**, 3448–3459
- Fleishman, S. J., Yifrach, O., and Ben-Tal, N. (2004) *J. Mol. Biol.* **340**, 307–318
- Fleishman, S. J., Unger, V. M., Yeager, M., and Ben-Tal, N. (2004) *Mol. Cell* **15**, 879–888
- Yeager, M., and Gilula, N. B. (1992) *J. Mol. Biol.* **223**, 929–948
- Aasen, T., Hodgins, M. B., Edward, M., and Graham, S. V. (2003) *Oncogene* **22**, 7969–7980
- Evans, W. H., and Martin, P. E. (2002) *Mol. Membr. Biol.* **19**, 121–136
- Carter, P. J., Winter, G., Wilkinson, A. J., and Fersht, A. R. (1984) *Cell* **38**, 835–840
- Nikolova, P. V., Wong, K. B., DeDecker, B., Henckel, J., and Fersht, A. R. (2000) *EMBO J.* **19**, 370–378
- Horovitz, A., Bochkareva, E. S., Yifrach, O., and Girshovich, A. S. (1994) *J. Mol. Biol.* **238**, 133–138
- Horovitz, A., Bochkareva, E. S., Kovalenko, O., and Girshovich, A. S. (1993) *J. Mol. Biol.* **231**, 58–64
- Horovitz, A., Serrano, L., Avron, B., Bycroft, M., and Fersht, A. R. (1990) *J. Mol. Biol.* **216**, 1031–1044
- Hendsch, Z. S., and Tidor, B. (1994) *Protein Sci.* **3**, 211–226
- Numakura, C., Lin, C., Ikegami, T., Guldberg, P., and Hayasaka, K. (2002) *Hum. Mutat.* **20**, 392–398
- Fleishman, S. J., and Ben-Tal, N. (2006) *Curr. Opin. Struct. Biol.* **16**, 496–504
- Das Sarma, J., Meyer, R. A., Wang, F., Abraham, V., Lo, C. W., and Koval, M. (2001) *J. Cell Sci.* **114**, 4013–4024
- VanSlyke, J. K., Deschenes, S. M., and Musil, L. S. (2000) *Mol. Biol. Cell* **11**, 1933–1946
- Ressot, C., Latour, P., Blanquet-Grossard, F., Sturtz, F., Duthel, S., Battin, J., Corbillion, E., Ollagnon, E., Serville, F., Vandenberghe, A., Dautigny, A., and Pham-Dinh, D. (1996) *Hum. Genet.* **98**, 172–175
- Roisman, L. C., Piehler, J., Trosset, J. Y., Scheraga, H. A., and Schreiber, G. (2001) *Proc. Natl. Acad. Sci. U. S. A.* **98**, 13231–13236
- Dall'Acqua, W., Goldman, E. R., Lin, W., Teng, C., Tsuchiya, D., Li, H., Ysern, X., Braden, B. C., Li, Y., Smith-Gill, S. J., and Mariuzza, R. A. (1998) *Biochemistry* **37**, 7981–7991
- Marlin, S., Garabedian, E. N., Roger, G., Moatti, L., Matha, N., Lewin, P., Petit, C., and Denoyelle, F. (2001) *Arch. Otolaryngol. Head Neck Surg.* **127**, 927–933
- Kenna, M. A., Wu, B. L., Cotanche, D. A., Korf, B. R., and Rehm, H. L. (2001) *Arch. Otolaryngol. Head Neck Surg.* **127**, 1037–1042
- Mese, G., Londin, E., Mui, R., Brink, P. R., and White, T. W. (2004) *Hum. Genet.* **115**, 191–199
- Gottfried, I., Landau, M., Glaser, F., Di, W. L., Ophir, J., Mevorah, B., Ben-Tal, N., Kelsell, D. P., and Avraham, K. B. (2002) *Hum. Mol. Genet.* **11**, 1311–1316
- Kraulis, P. J. (1991) *J. Appl. Crystallogr.* **24**, 946–950
- Merritt, E. A., and Bacon, D. J. (1997) *Methods Enzymol.* **277**, 505–524